Journal of Functional Materials and Biomolecules

Journal homepage: www.shcpub.edu.in
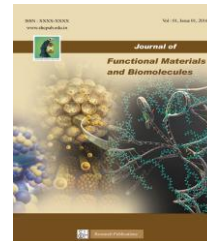
A Single-domain approach to simulate the effect of convective flow on the mushy-zone structure in Czochralski growth of gadolinium gallium garnet crystal

Reza Faiez[1] and Yazdan Rezaei[1]*

ABSTRACT

A numerical study was carried out to describe the effect of the melt hydrodynamics on the crystallization front shape in the Czochralski growth of a semitransparent oxide crystal. In the present model calculation, the enthalpy-porosity method was used to solve the phase change problem with the convection due to buoyant, thermocapillary and centrifugal forces. It was shown that the rotationally-driven flow protrudes into the mushy zone when the crystal rotation rate was increased to a certain critical value corresponding to $Gr/Re^2=0.89$ as the ratio between the intensity of buoyancy and forced convection flow in the melt.The ratio between the vertical and horizontal temperature gradients beneath the mushy zone was found to be decreased by increasing the crystal rotation rate.It was shown that the shape of the zone deforms abruptly when the ratio between the axial and radial temperature gradients decreased to the values smaller than the unity. The Burger's number condition was found to be violated in the case $Gr/Re^2<0.89$, at which the onset of geostrophic instability is expected.

Keywords: Enthalpy-porosity model;Czochralski growth; Numerical simulation; Hydrodynamic stability; Radiative heat transfer.

1 Introduction

Oxide single crystals are conventionally grown by the Czochralski (Cz) method primarily characterized by hydrodynamics of the melt which is inextricably coupled to transport phenomena in the melt. The Cz melt is in fact a good example of situation in which the fluid motion is brought about by different coexisting mechanisms, that is, heating from side (the crucible wall) yields a convective flow of the Hadley type, whereas cooling from above (the melt/gas interface and the crystal/melt boundary) may lead a Rayleigh-Benard type convection in the system [1]. Motions relevant to the Cz melt can be classified by the principle of driving forces into the following main groups: (a) gravitational (natural convection), (b) mechanical (forced convection), and (c) surface-tension (Marangoni convection). These different kinds of the melt motion determine the structure of the flow, the heat and mass transport in the fluid, the crystal-melt interface shape, and consequently the quality of the growing crystal.

In a Cz melt model, the ratio between the buoyancy and the rotationally-driven forces, denoted by Gr/Re2, is generally assumed as the non-dimensional parameter governing the convective interactions, and the flow is supposed to become unstable whenever its value approaches to acritical one around the unity. It has been shown that refractory oxides may exhibit an abrupt change in the interface shape, from a convex-to-melt phase boundary to a flat or even concave one, during the growth process [2-6]. This sudden and uncontrollable change is usually assigned to a critical value of the ratio Gr/Re2 in the melt. However, the manner in which the crystal-melt interface is represented is a central feature of bulk crystal growth models in which thephase change problems with convection play a significant role. A self-consistent growth model requires that the interface geometry be computed as part of the solution to the transport problem, and the main challenge is the presence of a moving phase boundary involving a strong coupling of mass and heat transfer. From an algorithmic point of view, two methods are primarily employed for solving phase change problems with convection and computing the position of the crystal-melt interface. The first one (front-tracking methods) is based on a multi-domain approach anddefines a discrete moving surface to separate the interface between crystal and melt. The second category (diffuse-interface methods) is based on a single-domain approach where a system of momentum and energy equations is solved in the entire physical domain, andtreats the interface as a region (mushy zone) of finite thicknessacross which physical properties vary rapidly but continuously from one bulk value to the other [7]. In contrast to the front-tracking methods, such as the widely used isotherm method, in a single-domain approach the thickness of the so-called mushy zone is very large compared to the width of a phase boundary of one or two layers of computational cells [8]. The main advantage of this approach is that the interface is not explicitly computed and the energy balance condition is automatically satisfied at the crystal-melt

* Corresponding author: rfaiez@gmail.com,
[1] Solid State Lasers Research Group, Lasers and Optics Research School, Tehran, P.O.Box 11365-8486, Iran.

Original Research Article

14 *J. Funct. Mater. Biomol. 1 (2017) 13–18*   *Reza Faiez et.al.*

interface.Voller and Prakash [9] have argued that when the material is not a pure substance, the phase transition occurs over a temperature range around the melting point. That is, the evolution of latent heat has a functional relationship with temperature as opposed to the step change associated with an isothermal phase change. In such cases, the phase transition takes place through the so-called mushy region, in which the fluid flowplays an important role in the final solidified microstructure.This numerical approach to solve the convection-diffusion controlled mushy region phase change problems is called the enthalpy-porosity model which includes latent heat effects as a source term, and comprises a technique to ensure that the velocity field vanishes in the solid phase [10,11]. In the present study,the enthalpy-porosity model was used to describe the phase change problem involving convection and radiation in a Czoxide crystal growth configuration. In thisinvestigation, the finite volume approximation (FVM) is applied to discrete the governing equations on stationary grid mesh system incorporating enthalpy-porosity model to simulate the effect of rotationally-driven forces on the mushy region structure. Correlation between hydrodynamic stability of the flow and the mushy-zone structure is studied.We intended to show that the mushy-zone morphology would be considerably deformed at a critical value of the ratio between the buoyancy- and rotationally-driven forces.

2 Model description
2.1 Geometry, thermal and radiative properties

The schematic in Fig. 1 illustrate the geometry of the Cz growth configuration adopted in the present numerical simulation, wherethe crystal radius at the constant-diameter stage of the growth is r_x= 30 mm.The crystal to crucible radii ratio (r_x/r_c) is 0.5, and the aspect ratio AR=h_c/r_c is 2.0, where h_c =120 mm is the height of the crucible side wall. The height of the tri-junction point J, is kept at 125mm, while the height of the melt free surface at the crucible wall is h_l= 120 mm. The crucible side wall is at a constant temperature $T_c=T_{mp}+\Delta T_{max}$, where ΔT_{max}=67 K is the applied temperature difference between the crucible wall and the melting point of the material.The crucible wall is assumed to be an opaque and gray surface diffusely emitting and reflecting but not absorbing the thermal radiation. The crucible bottom is thermally insulated, and its surface has the same radiation transfer properties (ε=0.5) as the crucible side wall. Both the melt and the crystal have the same optical thickness, and they absorb and emit but not scatter radiation. Theoptical properties of the material (such as refractive index, n=1.8 and absorption coefficient, a=258 m^{-1}[6]) are independent of temperature and wavelength. Throughout this work, the melt-gas interface is assumed to be a semitransparent diffuse gray surface, which is slightly curved to form a meniscus configuration at the crystal periphery.
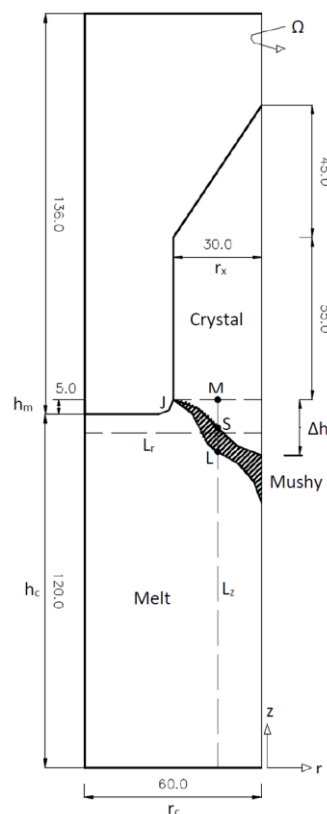
Fig. 1. Geometry of the Cz growth model with a hypothetical mushy region between the crystal and melt. Dashed horizontal line, Lr (5 mm below the melt free surface) and vertical line Lz , crossing the point M(r,z)= (rx/2, 125mm) are described. The point J is the tri-junction point, hm is the height of the melt meniscus region, and Δh is the convex to melt interface depth.

With the refractive index of the melt (and the crystal), the Spuckler-Siegel[12] approximation was used to estimate the transmissivites (τ_{ext}=0.85, and τ_{in}=0.23) on both sides of the melt free surface. The emissivity, ε at the crystal surface is assumed to be 0.3. Energy is transmitted through the free surface of the melt (and the crystal) to the ambient walls (ε=0.7) at $T_a\cong$1650K. The ambient gas is assumed to be totally transparent. The crucible is at rest, and the no-slip condition is applied to all physical boundaries of the melt except the melt-gas interface on which thermocapillary forces are taken into account. The crystal rotates uniformly around the symmetry axis. The crystal rotation rate, 0.5<Ω(rad/s)<3.0, is the only variable external parameter in the present model. In contrast to the front-tracking method where the interface shape coincides with the melting point isothermT_{mp}=2023K, the crystal-melt mushy zone is treated as a region of finite thickness across which the phase change occurs.

Table 1. Thermophysical properties including optical data employed in calculation. The subscribes l, x and c denote melt, crystal and crucible, respectively.

Description (units)	Symbol	Value
Melting point (K)	T_{mp}	2023
Dynamic viscosity ($g/cm \cdot s$)	η	0.40
Kinematic viscosity (cm^2/s)	ν	7.08×10^{-2}
Thermocapillary coefficient ($N/m \cdot K$)	$\gamma_T = -\partial\sigma_l/\partial T$	$\gamma_T = -2.76 \times 10^{-4}$
Thermal expansion coefficient (K^{-1})	β	$\beta_l = 2.7 \times 10^{-5}$
Density (g/cm^3)	ρ	5.65
Thermal conductivity ($W/m \cdot K$)	k	5.0
Heat capacity ($J/g \cdot K$)	$C_{p,l} = C_{p,x}$	0.586
Thermal diffusivity (cm^2/s)	$\alpha = (k/C_p\rho)$	1.51×10^{-2}
Refractive index	$n_l = n_x$	1.8
Absorption coefficient (m^{-1})	$a_l = a_x$	258
Transmissivity of melt surface	τ_{ext} and τ_{in}	0.85 and 0.23
Prandtl number	$Pr = \eta C_p/k$	4.69
Reynolds number	$Re = (r_c - r_x)^2 \Omega/\nu$	$(1.2712\times10^2)\Omega$
Grashof number	$Gr = (g\beta/\nu^2)\Delta T_{max} r_c^3$	7.646×10^4
Marangoni number	$Ma = (\gamma T/\eta\alpha)\Delta T_{max} r_c$	1.837×10^4
Thermal Rossby number	$Ro_T = g\beta(\Delta T/\Delta z)h_c^2/\Omega^2(r_c - r_x)^2$	$Ro_T = 0.424(\Delta T/\Delta z)/\Omega^2$

2.2 Dimensionless parameters

The thermophysical properties of the material (gadolinium gallium garnet) employed for the present calculations, and the dimensionless parameters which describe the convective flow in the melt are listed in Table 1. The oxide ($Gd_3Ga_5O_{12}$) melt is characterized by the Prandtl number $Pr \cong 4.69$, the Grashof number $Gr=1.141\times10^3\Delta T_{max}$, the Reynolds number $Re=1.271\times10^2\Omega$, and the Marangoni number $Ma= 2.742\times10^2\Delta T_{max}$, where Ω(rad/s) is the crystal rotation rate and $\Delta T_{max}=67K$ is the driving temperature difference which ensures the growth ofcrystal at the tri-junction point, J(r,z)=(30mm, z=125mm). For the present mixed convection problem, the ratio between buoyancy and the rotationally-driven forces is given by $Gr/Re^2=4.732/\Omega^2$, and the critical Reynolds number is approximated by $Re^* \cong Gr^{1/2}$, at which ($Re^* \cong 276.5$) the intensity of forced convection flow is comparable to that of the buoyancy-driven one. In a Cz melt model, and particularly in the column of the flow beneath the phase boundary, both density variations (thermal stratification) and the crystal rotation rate are intrinsic to the hydrodynamic stability of flow. As a measure of the relative importance of thermal stratification and the rotationally-driven effects, the Burger number, Bu is used to predict the breakdown of axisymmetry with the onset of the geostrophic instability if the condition Bu < Bu*= 0.58 is fulfilled. In the present Cz model (AR=2.0), the Burger number can be expressed by $Bu=(N/\Omega)^2$, where $N=(g\beta\partial T/\partial z)^{1/2}$ is the buoyancy frequency with which an adiabatically displaced fluid particle will oscillate about its equilibrium position [1]. The condition (Bu<Bu*) is satisfied whenever the crystal rotation rate exceeds a critical value at which the convective flow is characterized by $Gr/Re^2 \leq 0.89$.The most direct measure of the relative importance of the density and velocity gradients is provided by the gradient form of the Richardson number,

Rig, which can be expressed as Rig=4Bu/(RoT)2[13],where RoT is the thermal Rossby number.Fein and Pfeffer [13]have reported that, for all the experimental cases studied (Pr<1, and Pr>1), Rig increases as the rotation rate is increasing.

2.3 Mathematical model

Assuming that the Cz/oxide melt is Newtonian and incompressible, the enthalpy-porosity governing equations [9-11] can be expressed as

Conservation of momentum:
$$\rho\frac{\partial u}{\partial t} + \rho u.\nabla u = -\nabla p + \eta\nabla^2 u + Au + S(H) \quad ....(1)$$

Conservation of mass:
$$\nabla.u = 0 \quad ....(2)$$

Conservation of energy:
$$\frac{\partial H}{\partial t} + u.\nabla H - k\nabla^2 T + \nabla.q_R = 0 \quad ....(3)$$

where u(x,t)is the flow velocity vector at any point x(r,z) and at any time t, p is the pressure, H is the enthalpy, q_R is the radiation heat flux through the melt.A is defined so that the momentum equations are forced to mimic the Carman-Kozeny equation [10]

$$\nabla_P = \frac{-C(1-\lambda)^2}{\lambda^3 u} \quad ....(4)$$

which suggests the following form for the function A in the momentum equation,

$$A = \frac{-C(1-\lambda)^2}{(\lambda^3 + b)} \quad ....(5)$$

where the factor b is a small constantvalueintroduced to avoid division by zero, C is a constant accounting for the mushy-zone morphology, and λ is the porosity which takes the values, $\lambda=1$in the liquid phase, $\lambda=0$ in the solid phase, and $0<\lambda<1$ in the mushy region. The equation (5) implies that, A vanishes in the fluid and has no influence in the

liquid phase. In the solid phase, however, A takes a large value and forces the velocity field to be vanished.

Assuming the Boussinesq approximation to be valid, that is, density is constant in all terms except a gravity source term, that buoyancy source term can be expressed as

$$S(H) = \frac{g\beta(H - H_{ref})}{C_p} \quad\text{............................(6)}$$

where g=(0,0,-g)is the accelerationvector due to gravity,β is the thermal expansion coefficient, c_p is the specific heat of the material, H_{ref} is a reference value for the enthalpy, and the enthalpy of the material (the total heat constant) is given by

$$H = \rho\Delta H_f + \rho C_p T_{mp} + \rho C_p(T - T_{mp}) \quad\text{.............................(7)}$$

where ΔH_f is the latent heat of fusion. To estimate the radiative heat flux, q_Rin Eq.(3), we have to solve the radiative transfer equation. In the present study, the Sn-type (S4) discrete ordinates (DO) method [14], based on a discrete representation of the angular dependence of the radiation intensity, was used. The balance of energy passing in a specified direction Ω through a small differential volume in an axisymmetric system is given by the following equation when the scattering is ignored:

$$\frac{\mu_m}{r}\left[\frac{\partial(rI_m)}{\partial r}\right] - \frac{1}{r}\left[\frac{\partial(\eta_m I_m)}{\partial\phi}\right] + \zeta_m\frac{\partial I_m}{\partial z} = -aI_m + aI_m \quad\text{..............................(4)}$$

where μ_m,η_m and ζ_m are the direction cosines and I_m is the intensity of radiation for the discrete direction Ω_m. ϕ is the angle of revolution around the z-axis, and I_b is the intensity of blackbody radiation at the temperature of medium. The absorption coefficient of the melt (and the crystal), is denoted by a. The radiative heat flux, q_Rcan be expressed as follows:

$$q_R = \sum_m \omega_m \Omega_m I_m \quad\text{.............................(5)}$$

where ω_m is angular quadrature weight which sums to the surface area of unit sphere, and the index, m is used to sum over all directions.

We applied the finite volume technique (FVM) to compute steady and axisymmetric solutions to the fully coupled equationsgoverning the convective flow involving solidification in the Cz growth system represented in Fig. (1). The SIMPLE algorithm was used to couple velocities and pressure on staggered grids, and second order upwind method was used for discretization of momentum and energy equations. The equations are integrated over each control volume (CV) and resulting system of algebraic equations was solved iteratively until convergence was reached. Non-uniform finite volume mesh structure used to perform the calculations in this work, consists of 36446 mixed (quadrilateral and triangular) cells. According to the investigations of Voller and Prakash [9], the constants b andC in the equations (4) and (5) are set at 10-3 and 1.6×105, respectively. The numerical results in the next section implies that the chosen value of C is small enough to allow for significant flow in the mushy region whereas the limiting value of the function A, that is, A=-C/λis large

enough to suppress the flow velocity field in the solid phase.

3 Results and Discussion

Steady-state simulations of the convective flow pattern and temperature field are represented in Fig.2(a,b,c).These figures are relevant to three different crystal rotation rates, i.e., Ω= 1.5, 2.0, and 2.5rad/s corresponding to Gr/Re^2=2.10, 1.18, and 0.75, respectively.The general feature of the fluid motion is described as following. The buoyancy-driven hot flow ascends along the crucible side wall and then, accompanied by the thermocapillary flow, travels along the melt free surface towards the crystal rim. Due to the convection and radiation at the melt free surface, the fluid is being cooled down along the path,and this creates a stream of cold fluid which descends along the melt centerline towards the crucible bottom.Due to the optical properties of the melt, the flow does not exhibit undulating structure observed in high Prandtl number opaque melts [3].However, owing to the relatively large optical thickness of the fluid, the isotherms are more squeezed at the corner, and the vortex centerof thermal convection flow is located at a position lower than the melt middle. When the rotation rate is smaller than ~2.3 rad/s, the flow is essentially a buoyancy-driven one with a large, unicellular counter-clockwise circulation. Increasing in the rotation rate to ~2.5 rad/s, small rotationally-driven, clockwise cells appear in the vicinity of the crystallization front and nearby the crucible bottom.
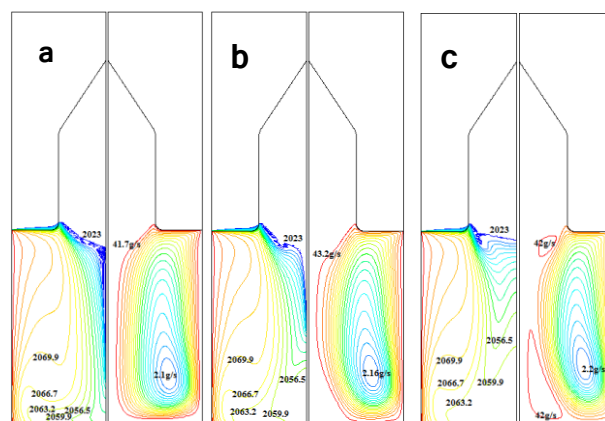
**Fig.2.**Contour plots of isotherms (left side) and stream function (right side) in the semitransparent melt (a_l x r_c=15.48) for different rotation rates: (a) Ω=1.5, (b) Ω=2.0, and (c) Ω=2.5 rad/s.

As shown in Fig.2(a,b,c), in the cases with (Gr/Re^2)>1.18, the flow pattern is associated by a convex-to-melt interface, which tends to be nearly flat when the rotation rate is increased to 2.5 rad/s, corresponding to Gr/Re^2=0.75. In Fig.2(a), the isotherms close to the phase boundary are regular and more density of heat flux lines implies that the heat transfer is intensified along the interface. In this case the isotherms T(1)=2056.5K and T(2)=2060K both are found to be reached the crucible bottom. Fig.2(b) shows that increasing the rotation rate

from 1.5 to 2.0, the regular shape of the isotherms in the vicinity of the interface is changed at around the interface mid-point, r=15mm, and more density of lines are located between meniscus region of the melt and the convex-to-melt interface mid-point. In this case, the isotherm T(1) turns toward the axis while T(2) reaches to the crucible bottom. Further increase in the rotation rate (from 2.0 to 2.5 rad/s) results in a nearly flat interface. As shown in Fig.2(c),the isotherms are more squeezed in the meniscus region, and they are strongly deformed along the rest of the interface.In this situation both of the isotherms T(1) and T(2) are found to be turned and reached to the symmetry axis. These results are consistent with the well-known [15] effect of the melt meniscus at the crystal periphery which allows for radial heat transfer (both convective and radiative)from the melt to surrounding near the crystallization front and reduces the net radial heat transfer from the melt to the interface.This effect leads to decrease in the convexity of the interface.
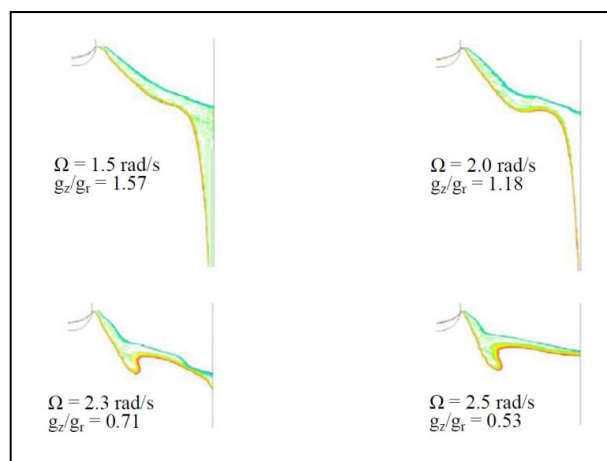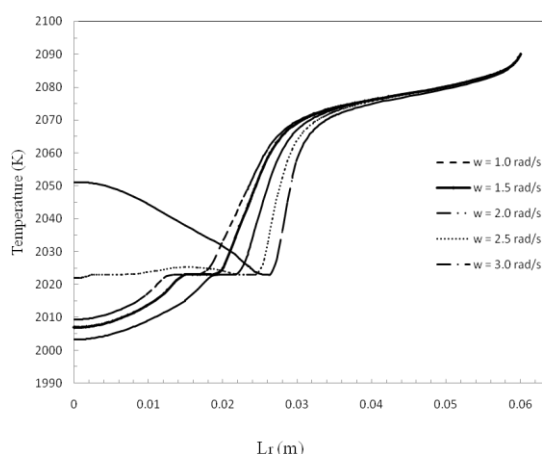

Fig.3. Effect of the crystal rotation rate on the mushy-zone morphology. The ratio between the axial and radial temperature gradients decreases with increasing rotation rate.

The effect of rotationally-driven forces on the morphology of mushy-zone is represented in Fig. 3. Note that the ratio between the axial and horizontal temperature gradients, g_z/g_r decreases with increasing the crystal rotation rate, and the mushy region was found to be strongly deformed when (g_z/g_r) beneath the phase boundary decreased to the values smaller than unity(i.e., in the cases with $\Omega \geq 2.3$ rad/s). Fig. 3 shows that the convex-to-melt interface at Ω=1.5 rad/s is changed to form a "*gull-wing*" geometry at Ω=2.0 rad/s.The effect of rotation rate on the radial velocity profile along the horizontal line, L_r is illustrated in Fig. 4. The line L_r(5mm below the melt free surface) is crossing the mushy region (0<r(mm)<30). Fig. 4 shows that the convective flow protrudes into the zone, and the velocity profile was found to be changed for the cases $\Omega \geq 2.0$ rad/s. In other words, when $\Omega \leq 2.0$rad/s, the fluid motion within the mushy-zone is dominated by the buoyancy and thermocapillary forces (u_r<0). The sign of the velocity component, which was altered at the rotation
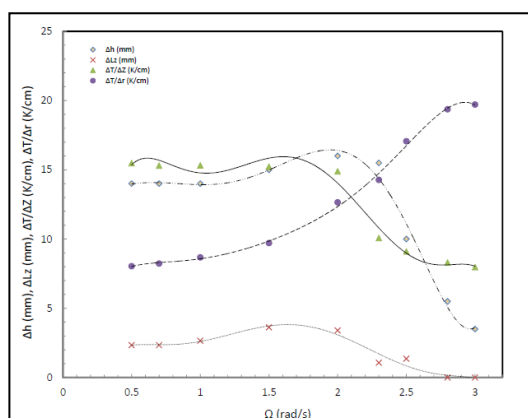
rates even slightly greater than 2.0 rad/s (e.g., Ω=2.3 rad/s, corresponding to Gr/Re^2=0.89), implies that the forced convection flow plays a significant role in deformation of the mushy-zone morphology. Correspondingly, the effect of rotation rate on the temperature profile along the same horizontal line (L_r) is depicted in Fig. 5. It is shown that the crystallization front (0<r(mm)<30) tends to be flat at Ω=2.5 rad/s, and this can be inferred that the interface–inversion process occurs at Ω=2.8-3.0 rad/s. It is worthy to note (but not shown here) that, the flow field found to be dominated by the rotationally-driven forces when the rotation rate increased from 2.5 to 2.8 rad/s at which a large cold plume appearsbeneath the mushy-zone and, descending along the symmetry axis toward the crucible bottom, tends to break away from the axial position and the flow direction.The effect of rotation rate on the interface depth (Δh), the thickness of the mushy region (ΔL_z) at r=r_x/2, and the averaged axial and radial temperature gradients in the melt beneath the interface is illustrated in Fig. 6. It is shown that the $g_r$increases, and $g_z$decreases first (0.5<Ω(rad/s)<2.0) slowly and then (Ω>2.0 rad/s) more rapidly with increasing rotation rate. The depth of the crystallization front was found to be sharply decreased for the cases Ω>2.0 rad/s (Re>254.24 and Gr/Re^2<1.18) which corresponds to $(g_z/g_r)\leq1.0$. The morphology of mushy-zone depends on the rotationally-driven forces which affects g_z/g_rin the Cz melt. As expected [13], Fig. 7 shows that the gradient Richardson number(Ri_g) increases and the thermal Rossby number (Ro_T) decreases as the forced convection flow, represented by the Reynods number (Re), is intensifying. It is shown that, increasing the rotation rate from 2.0 to 2.3 rad/s the governing parameter of mixed convection (Gr/Re^2) decreases from 1.18 to a value lower than unity (i.e., 0.89). Consistently,Ro_Tdecreases from 1.59 to 0.81in the case with Ω=2.3 rad/s at which the Burger number is equal to its critical value (Bu^*=0.58) [1,13], and the morphology of the mushy region was found to be clearly modified.
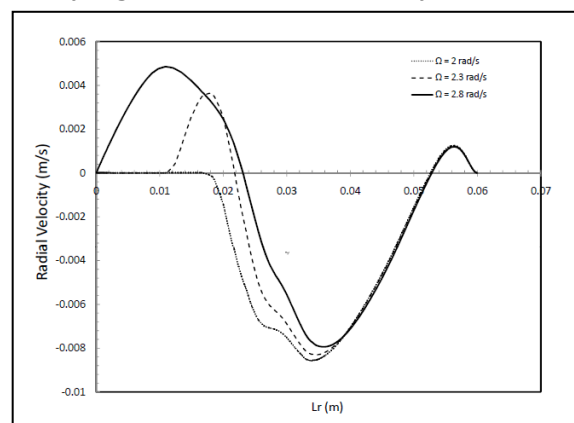

Fig. 4. Effect of rotation rate on the radial velocity profile along the horizontal line L_r (5mm below the melt free surface), crossing the mushy region. The mixed convection flow penetrates into the mushy zone, and for the cases Ω>2.0 rad/s, the rotationally-driven flow protrudes in the crystal-melt region and affects the morphology of the zone.

Original Research Article

18 *J. Funct. Mater. Biomol. 1 (2017) 13–18*   *Reza Faiez et.al.*

4 Conclusions

The enthalpy-porosity method developed by Voller and Prakash [9,10] was used to solve the phase-change problem involving mixed convection and radiation in a Czochralski crystal growth model. A finite volume (FVM) method was applied to compute two-dimensional and axisymmetric solutions to the fully coupled equations governing the melt hydrodynamic and heat transfer in the model, and discrete ordinates method (DOM) was used to account for the influence of internal radiative heat transfer on the flow field and the temperature distribution in the material. The effect of rotationally-driven forces on the structure of the mushy region was studied. It was shown that the morphology of mushy-zone depends on the ratio between the axial and radial temperature gradients (g_z/g_r), which decreases as the crystal rotation rate increased. The mushy-zone structure was found to be correlated with the hydrodynamic stability of the flow.

Fig. 5. Effect of rotation rate on the temperature profile along the horizontal line, L_r (5mm below the melt free surface) crossing the mushy region.

Fig. 6. Variation of the interface depth (Δh), the thickness of mushy zone (ΔL_z) at r=15mm, and the temperature gradients $\Delta T/\Delta z$ and $\Delta T/\Delta r$ with the crystal rotation rate.
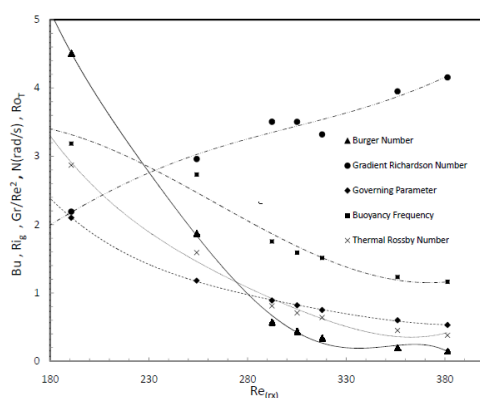
Fig. 7. Variation of the dimensionless parameters characterizing the hydrodynamic stability of the flow, each as a function the rotationally-driven flow intensity. The governing parameter of the mixed convection flow is given by Gr/Re^2, $Ri_g = N^2/(\partial u_r/\partial z)^2$ is the gradient Richardson number, $Bu = [(N/2\Omega)(h_c/r_c)]^2$ is the Burger's number, where N is the buoyancy frequency.

References

[1] J. R. Ristorcelli and J. L. Lumley, J. Cryst. Growth 116 (1992) 447-460.

[2] P. Hintz and D. Schwabe, J. Cryst. Growth 222 (2001) 356-364.

[3] Q. Xiao and J. J. Derby, J. Cryst. Growth 139 (1994) 147-157.

[4] M. Kobayashi, T. Hagino, T. Tsukada, and M. Hozawa, J. Cryst. Growth 235 (2002) 258-270.

[5] D. Schwabe, R. R. Sumathi, and H. Wilke, J. Cryst. Growth 265 (2004) 494-504.

[6] O. N. Budenkova, M. G. Vasiliev, V. S. Yuferev, I. A. Ivanov, A. M. Bulkanova, and V. V. Kalaev, Crystallog. Reports 53 (2008) 1181-1190.

[7] I. J. Derby, J. R. Chelikowsky, T. Sinno, B. Dai, Y.-I. Kwon, L. Lun, A. Pandy, and A. Yeckel, Large-scale numerical modeling of melt and solution crystal growth, 13th International Summer School on Crystal Growth, University of Pennsylvania, 139-158 (2007).

[8] M. Lappa, Fluids, Materials and Microgravity: Numerical Techniques and Insight into Physics, Elsevier, Amsterdam (2004).

[9] V. R, Voller and C. Prakash, Int. J. Heat Mass Transfer 30 (1987) 1709-1719.

[10] V. R. Voller, M. Cross, and N. C. Markatos, Int. J. Numer. Methods in Eng. 24 (1987) 271-284.

[11] Y. Belhamadia, A. S. Kane, and A. Fortin, Int. J. Numer. Analysis and Modeling, B 3 (2012) 192-206.

[12] C. M. Spuckler and R. Siegel, J. Thermodyn. & Heat Transfer 6 (1992) 596-604.

[13] J. S. Fein and R. L. Pfeffer, J. Fluid Mech. 75 (1976) 81-112.

[14] G. Colomer, Numerical Methods for Radiative Heat Transfer, Chapt. 3, Doctoral Thesis, UPC/ CTTCP, Catalunia (2006).

[15] R. K. Srivastava, P. A. Ramachandran, and M. P. Dudukovic, J. Cryst. Growth 73 (1985) 487-504.